iScience

CellPress
OPEN ACCESS

Article

Imaging Acute Metabolic Changes in Patients with Mild Traumatic Brain Injury Using Hyperpolarized [1-^{13}C]Pyruvate

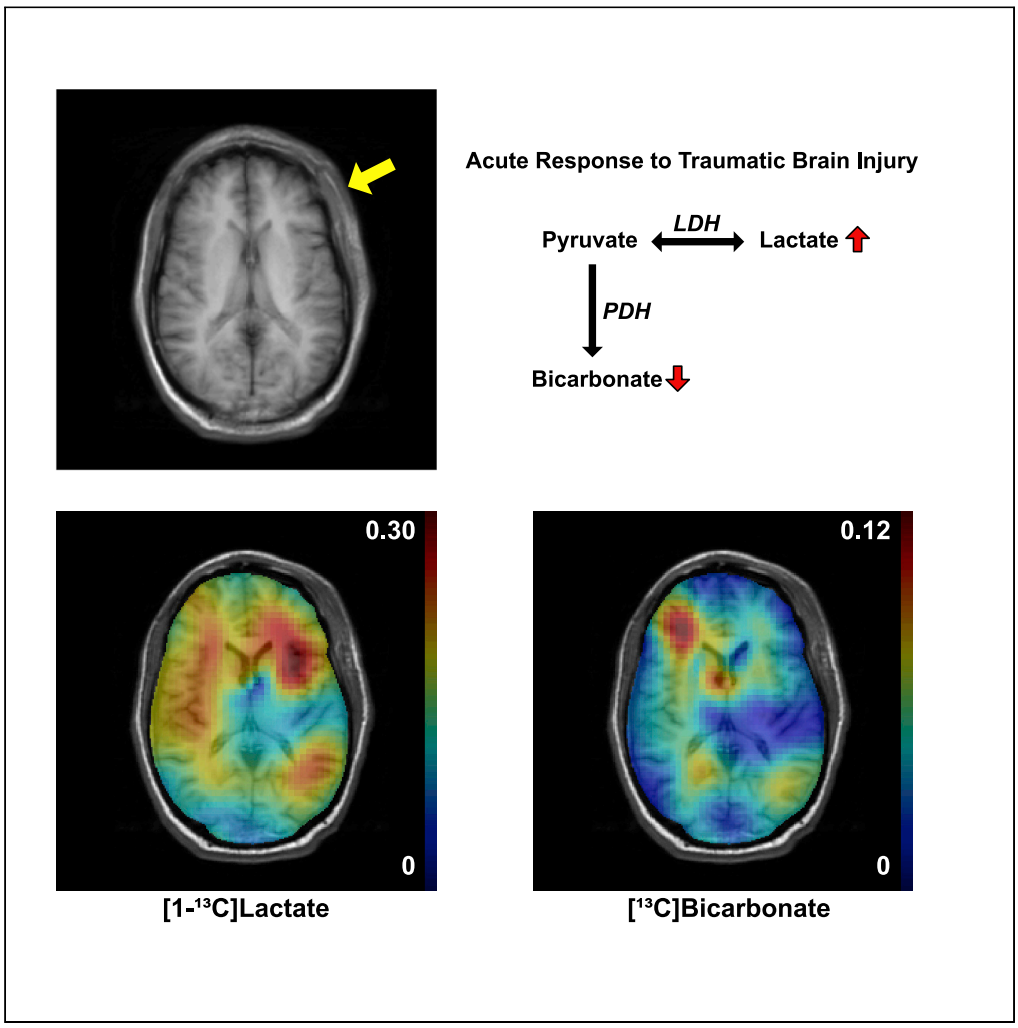

Edward P. Hackett, Marco C. Pinho, Crystal E. Harrison, ..., Surendra Barshikar, Christopher J. Madden, Jae Mo Park

jaemo.park@utsouthwestern.edu

HIGHLIGHTS

Clinical translation of hyperpolarized pyruvate to TBI was demonstrated

Patients with mild TBI were imaged with hyperpolarized [1-^{13}C] pyruvate

Altered lactate and HCO_3^- production in the brain nearest the site of trauma

Hackett et al., iScience *23*, 101885
December 18, 2020
https://doi.org/10.1016/j.isci.2020.101885

iScience

CellPress
OPEN ACCESS

Article

Imaging Acute Metabolic Changes in Patients with Mild Traumatic Brain Injury Using Hyperpolarized [1-^{13}C]Pyruvate

Edward P. Hackett,[1] Marco C. Pinho,[1,2] Crystal E. Harrison,[1] Galen D. Reed,[1,3] Jeff Liticker,[1] Jaffar Raza,[4] Ronald G. Hall,[4] Craig R. Malloy,[1,5] Surendra Barshikar,[6] Christopher J. Madden,[7] and Jae Mo Park[1,2,8,9,*]

SUMMARY

Traumatic brain injury (TBI) involves complex secondary injury processes following the primary injury. The secondary injury is often associated with rapid metabolic shifts and impaired brain function immediately after the initial tissue damage. Magnetic resonance spectroscopic imaging (MRSI) coupled with hyperpolarization of ^{13}C-labeled substrates provides a unique opportunity to map the metabolic changes in the brain after traumatic injury in real-time without invasive procedures. In this report, we investigated two patients with acute mild TBI (Glasgow coma scale 15) but no anatomical brain injury or hemorrhage. Patients were imaged with hyperpolarized [1-^{13}C]pyruvate MRSI 1 or 6 days after head trauma. Both patients showed significantly reduced bicarbonate (HCO_3^-) production, and one showed hyperintense lactate production at the injured sites. This study reports the feasibility of imaging altered metabolism using hyperpolarized pyruvate in patients with TBI, demonstrating the translatability and sensitivity of the technology to cerebral metabolic changes after mild TBI.

INTRODUCTION

Traumatic brain injury (TBI) causes mechanical damage and disruption of normal metabolism in the brain (Corps et al., 2015). A major challenge for clinicians is managing complex secondary processes following the primary injury. After the primary trauma, the surviving tissue undergoes metabolic shifts, resulting in the development of potentially hazardous secondary metabolites and further damage. The secondary events develop over a timescale after the primary injury, providing a potential window of opportunity for detection and therapeutic intervention. Moreover, TBI is suspected to contribute to a variety of chronic degenerative processes such as chronic traumatic encephalopathy, Alzheimer disease, and Parkinson disease (Smith et al., 2013). Numerous therapies have been proposed to reduce or prevent secondary brain damage, directly impacting long-term patient outcome (Xiong et al., 2015). Therefore, the noninvasive detection and characterization of TBI pathophysiology during the acute and sub-acute stages will have critical clinical implications and will be vital for identifying and developing effective therapies.

Altered glucose metabolism and mitochondrial dysfunction are features of the pathophysiologic events subsequent to TBI (Brooks and Martin, 2015; Kim et al., 2017). Invasive microdialysis methods have been reported to study brain metabolism in these patients, but in spite of the critical importance of directly detecting mitochondrial function, no specific noninvasive methods exist. Positron emission tomography (PET) detects uptake of radioactively labeled compounds such as glucose or acetate (e.g., [^{18}F]FDG, [^{11}C]acetate) in the human brain. Previous studies demonstrating cerebral hyperglycolysis in patients with TBI using [^{18}F]fluorodeoxyglucose ([^{18}F]FDG) PET measured cellular glucose uptake but could not measure the metabolic fate of glucose (Bergsneider et al., 1997). Another [^{18}F]FDG-PET study that combined with microdialysis of patients with TBI reported that the rate of glucose metabolism correlates with microdialysate lactate and pyruvate concentrations but not with the lactate-to-pyruvate ratio (Hutchinson et al., 2009), suggesting an increase in glucose metabolism to both lactate and pyruvate, as opposed to a shift toward anaerobic metabolism. Other studies indicated that the increased glucose uptake is directly related to the upregulated pentose phosphate pathway rather than to the rest of the glycolysis (Dusick et al., 2007).

[1]Advanced Imaging Research Center, The University of Texas Southwestern Medical Center, Dallas, TX 75390, USA

[2]Department of Radiology, The University of Texas Southwestern Medical Center, Dallas, TX 75390, USA

[3]GE Healthcare, Dallas, TX 75390, USA

[4]Department of Pharmacy Practice, The Texas Tech University Health Sciences Center, Dallas, TX 75216, USA

[5]Department of Internal Medicine, The University of Texas Southwestern Medical Center, Dallas, TX 75390, USA

[6]Department of Physical Medicine & Rehabilitation, The University of Texas Southwestern Medical Center, Dallas, TX 75390, USA

[7]Department of Neurological Surgery, The University of Texas Southwestern Medical Center, Dallas, TX 75390, USA

[8]Department of Electrical and Computer Engineering, The University of Texas at Dallas, Richardson TX 75080, USA

[9]Lead Contact

*Correspondence: jaemo.park@utsouthwestern.edu

https://doi.org/10.1016/j.isci.2020.101885

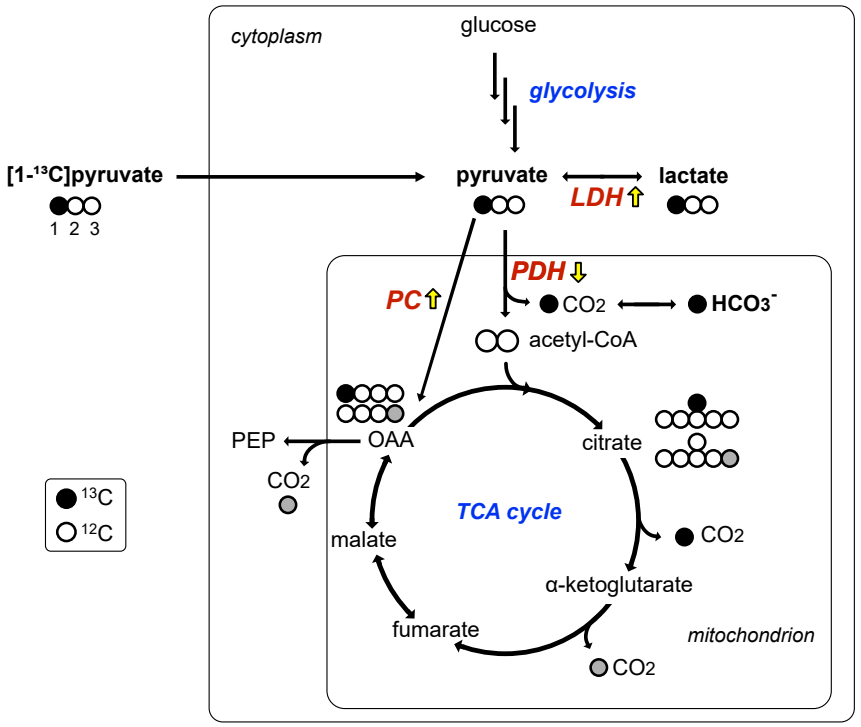

Figure 1. Metabolic Fate of Hyperpolarized [1-^{13}C]Pyruvate in the Brain

[1-^{13}C]Pyruvate (black circle: ^{13}C, white circle: ^{12}C) is converted either to [1-^{13}C]lactate via LDH or acetyl-CoA and $^{13}CO_2$ (and [^{13}C]HCO_3^-) through PDH. Possibly, [1-^{13}C]pyruvate can be also converted into [1-^{13}C]oxaloacetate (OAA) through PC, eventually releasing the labeled carbon (^{13}C) as CO_2. The gray circle indicates ^{13}C after backward scrambling of OAA to fumarate and malate in the TCA cycle. PEP: phosphoenolpyruvate; LDH: lactate dehydrogenase; PDH: pyruvate dehydrogenase; PC: pyruvate carboxylase.

Alternative way of imaging *in vivo* metabolism is using dynamic nuclear polarization (DNP) and rapid dissolution technique (Ardenkjaer-Larsen et al., 2003). Commercially available DNP polarizer can achieve more than 100,000-fold signal amplification of magnetic resonance-detectable (e.g., ^{13}C-labeled) substrates in liquid state. Administration of hyperpolarized ^{13}C-labeled substrates in coordination with ^{13}C magnetic resonance spectroscopy imaging (MRSI) opened new opportunities to assess *in vivo* metabolic processes of individual enzyme-catalyzed reactions in various organs including the brain. In particular, previous animal studies using hyperpolarized [1-^{13}C]pyruvate demonstrated that increased [1-^{13}C]lactate production in the injured brain tissue was associated with microglial activation (DeVience et al., 2017; Guglielmetti et al., 2017). Metabolites that are typically detectable in the cerebral ^{13}C spectrum using hyperpolarized [1-^{13}C]pyruvate are [1-^{13}C]lactate and [^{13}C]bicarbonate (HCO_3^-) as shown in Figure 1. The yellow arrows indicate metabolic shifts in acute TBI (DeVience et al., 2017). In this study, we translated these preclinical discoveries to demonstrate metabolic abnormalities in the brain of patients after acute mild TBI.

RESULTS

Two patients with acute TBI were recruited from the Parkland Health and Hospital System Emergency Room. Computed tomographic (CT) scans at admission confirmed that neither patient had underlying fractures, hemorrhage, or other anatomical injury. Patient #1 was a daily smoker, and Patient #2 was diabetic. Otherwise, both subjects were generally healthy and had no history of mental illness or alcoholism. Both patients tolerated the examination well.

The first patient was a 35-year-old African American male (88 kg, 168 cm) with a 2-cm laceration to the left frontal scalp due to blunt force trauma (whipped by a metal gun) with a Glasgow Coma Scale (GCS) score of 15 and no loss of consciousness (LOC). Figure 2 shows axial images of this patient 28 h after the head trauma. Besides left frontal scalp cutaneous edema/ecchymosis, no cerebral contusion or anatomical

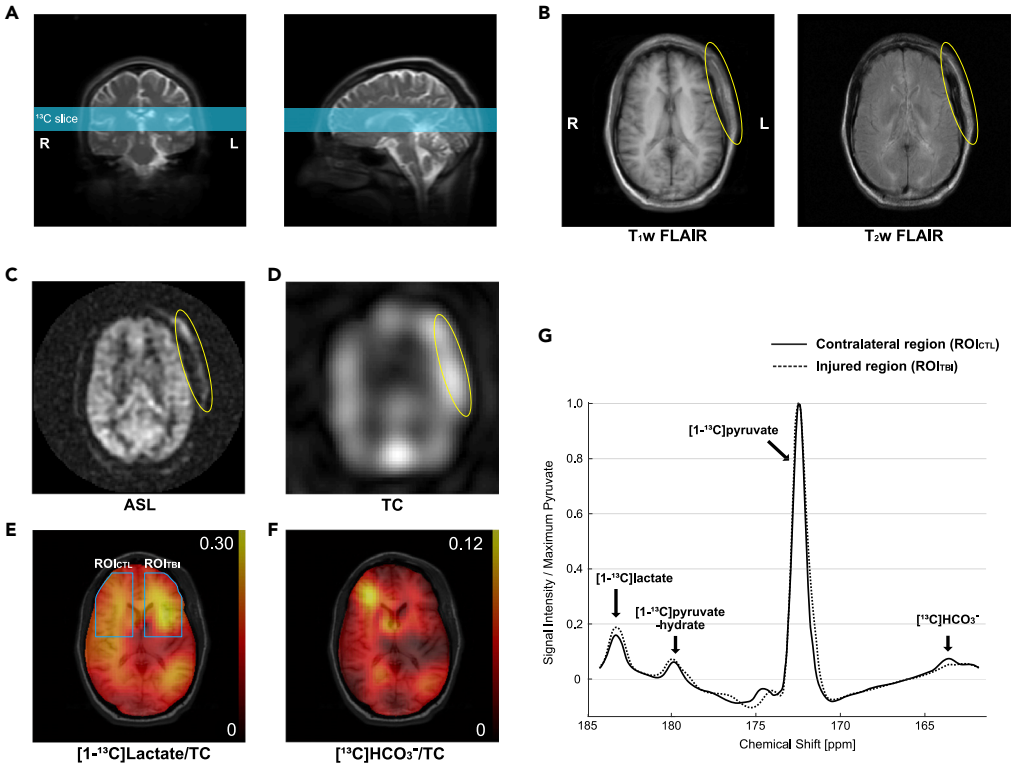

Figure 2. Metabolism of Acute TBI in Patient #1 Imaged by Hyperpolarized ^{13}C Pyruvate

The patient (35 years old, male), injured on the left frontal scalp (GCS 15, no LOC), was imaged 28 h after the injury.

(A) An axial slice that includes the injured region was prescribed for ^{13}C imaging.

(B and C) (B) T_1-weighted and T_2-weighted ^{1}H FLAIR and (C) ASL images showed swelling and increased perfusion in the injured site outside the skull (yellow circle), whereas no cerebral contusion, hemorrhage, or hypoperfusion was detected.

(D) Region with increased total hyperpolarized ^{13}C (TC) signal image matched to the scalp edema.

(E and F) (E) Increased [1-^{13}C]lactate conversion and (F) decreased [^{13}C]HCO_3^- production were detected in the brain tissues of the injured hemisphere.

(G) Averaged spectra over the injured brain region (ROI_{TBI}, dotted spectra) and the contralateral normal-appearing brain region (ROI_{CTL}, solid spectra).

brain damage was identified in the T_1-weighted and T_2-weighted fluid-attenuated inversion recovery (FLAIR) images. Arterial spin labeling (ASL) detected a hyperintense region at the site of the left frontal scalp injury but unremarkable appearance of cerebral perfusion. Likewise, total hyperpolarized ^{13}C signal was hyperintense in the injured scalp (Figure 2D) but comparable between the left and right brain hemispheres. In contrast, [^{13}C]HCO_3^- and [1-^{13}C]lactate production from hyperpolarized [1-^{13}C]pyruvate was altered in the injured side of the brain (left frontal lobe, underlying the scalp injury) when compared with the contralateral side (Figures 2E and 2F). [^{13}C]HCO_3^- signal, averaged over the injured region of interest and normalized with total ^{13}C (TC) signal (ROI_{TBI}, HCO_3^-/TC = 0.027), was 54.0% lower than that in the contralateral ROI (ROI_{CTL}, HCO_3^-/TC = 0.059). Conversely, lactate production in the injured region (lactate/TC = 0.236) was larger by 23.7% than the unimpacted contralateral brain region (lactate/TC = 0.191).

The second patient (Patient #2; 48 years old, 77 kg, 160 cm, Hispanic, male) sustained a head injury as a consequence of an ~6-m fall from a construction site scaffolding (GCS 15, 2 min LOC). When recruited, he had a 2-cm laceration to the left medial eyebrow and 5-cm subcutaneous hematoma extending laterally from the laceration. He was studied using the same ^{1}H/^{13}C magnetic resonance imaging (MRI) protocol 6 days after the initial injury. Similar to Patient #1, no structural brain damage was found in the ^{1}H MRI, but smaller [^{13}C]HCO_3^- was observed in the injured region (HCO_3^-/TC = 0.025) than the contralateral side of the brain (0.047) (Figure 3). [1-^{13}C]Lactate level was comparable (lactate/TC = 0.164 for the injured region and 0.162 for the contralateral region).

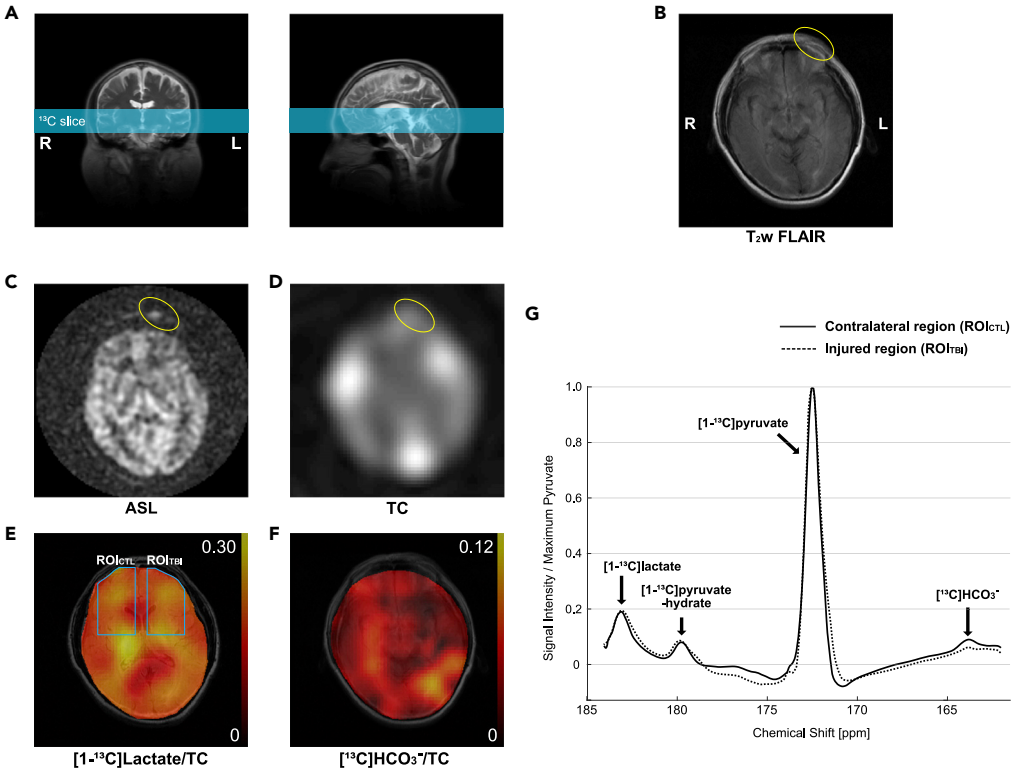

Figure 3. Hyperpolarized ^{13}C Pyruvate Imaging of Patient #2

The patient had a 2-cm laceration to the left medial eyebrow and 5-cm hematoma extending laterally from the laceration from a head injury (GCS 15, 2 min LOC). Images were acquired 6 days from the injury.

(A–C) (A) ^{13}C slice was prescribed to include the laceration. Axial ^{1}H images of (B) T_2-weighted FLAIR and (C) ASL showed the injured region outside the skull (yellow circle).

(D) Besides the scalp hematoma, no abnormal distribution of total hyperpolarized ^{13}C signals (TC).

(E and F) (E) Lactate was comparable between the impacted region and the contralateral side of the brain, whereas (F) decreased HCO_3^- signal was observed in the impacted brain region.

(G) Averaged spectra over the injured brain region (ROI_{TBI}, dotted spectra) and the contralateral normal-appearing brain region (ROI_{CTL}, solid spectra).

DISCUSSION

A common feature reported in patients with TBI is the increase of glucose consumption rate with no parallel increase in mitochondrial oxidative phosphorylation, known as hyperglycolysis (Bergsneider et al., 1997). Hyperglycolysis coupled with mitochondrial dysfunction should favor metabolism of pyruvate, the end product of glycolysis, to lactate via lactate dehydrogenase, rather than oxidation to acetyl-CoA via pyruvate dehydrogenase (PDH). The hyperintense [1-^{13}C]lactate signal in the impacted region from Patient #1 is consistent with previous *in vivo* preclinical imaging studies. DeVience et al. showed significant increase of [1-^{13}C]lactate production from hyperpolarized [1-^{13}C]pyruvate 4 h post-injury using a controlled cortical impact rat model (DeVience et al., 2017), and Guglielmetti et al. reported longitudinal changes of lactate production using this technique (Guglielmetti et al., 2017). The absence of hyperglycolysis in Patient #2 could be due to the severity of the injury (Bergsneider et al., 1997) or metabolic transition from hyperglycolysis to hypometabolic stage (Greco et al., 2020; Jalloh et al., 2015).

Mitochondrial dysfunction plays a key role in the pathophysiology of TBI (Kim et al., 2017). [^{13}C]HCO_3^- production from hyperpolarized [1-^{13}C]pyruvate reflects PDH flux. As PDH is an enzyme complex that is integrated into the inner membrane of the mitochondria, the decreased [^{13}C]HCO_3^- production in the injured brain region implies mitochondrial injury/dysfunction in spite of normal anatomy, which is consistent with previous animal study (DeVience et al., 2017). It should be noted that [^{13}C]HCO_3^- can be also produced via an anaplerotic pathway into the tricarboxylic acid cycle, which is exclusively achieved by pyruvate carboxylase (PC), an astrocyte-specific enzyme (Shank et al., 1985), as shown in Figure 1. Pyruvate carboxylation in

astrocyte increases during the secondary injury process, whereas pyruvate utilization via PDH is downregulated to protect neurons (Bartnik-Olson et al., 2013).

As shown in the Figures 2D and 3D, hyperpolarized ^{13}C signals were predominant in the gray matter rather than the white matter or subcutaneous tissues. These are consistent with previous human brain studies using hyperpolarized pyruvate (Gordon et al., 2019; Lee et al., 2019). Besides the directly impacted brain regions, the lactate and HCO_3^- maps showed larger variation in the patients when compared with those acquired from healthy subjects in previous studies. For instance, reduced HCO_3^- production was observed in the right posterior brain region of Patient #1, indicating possible contrecoup injury in the region.

Both patients were overweight. Patient #1 was very muscular with body mass index (BMI) of 31.2 but did not have a diagnosis of type 2 diabetes and was not on any hypoglycemic medications. Patient #2 (BMI = 30.1) did have a diagnosis of type 2 diabetes on metformin (500 mg orally twice daily). Plasma glucose levels of the patients were well within 160 mg/dL (108 for patient #1, 133 for patient #2), which is representative of normal brain biochemistry for clinical purposes as measured by PET (Varrone et al., 2009; Viglianti et al., 2017). Although diffuse changes in pyruvate metabolism could be postulated due to hyperglycemia, it seems unlikely that regional abnormalities as observed here would occur.

The specific timing of this glucose dysmetabolism is currently not known. Longitudinal monitoring with a larger patient population will be needed to further evaluate the utility of hyperpolarized pyruvate for noninvasive assessment of the TBI metabolism. If this result can be verified, it would have a major impact on the evaluation of patients involved in sports, military activities, or those who suffer from assault or accidents. Considering that this technique is safe and well-tolerated by patients, this technology may prove valuable for managing patients experiencing secondary injury processes, identifying early treatment response, and accelerating drug development efforts. In fact, pyruvate has been suggested as a neuro-protective substrate with therapeutic effect (Moro et al., 2016). Patients with moderate and severe TBI are expected to have larger metabolic alteration with potential challenges of imaging data interpretation due to morphological distortion and hemorrhage. Beyond acute and sub-acute TBI, the imaging methods and associated biomarkers to be developed under this application will be likely also applicable to concussion.

In this study, we investigated cerebral metabolism in patients with acute TBI using hyperpolarized [1-^{13}C] pyruvate. We found altered cerebral metabolism in the brain nearest the site of trauma despite no visible anatomical damage in the brain on MRI, demonstrating the sensitivity of hyperpolarized pyruvate to altered metabolism in TBI. The acute metabolic changes in [1-^{13}C]lactate and [^{13}C]HCO_3^- images in the injured region indicate the potential clinical utility of hyperpolarized [1-^{13}C]pyruvate in managing patients with TBI and provides objective evidence of injury even when conventional studies with CT and MRI are unrevealing.

Limitations of the Study

This study demonstrated the feasibility of hyperpolarized [1-^{13}C]pyruvate for imaging metabolic changes following a mild brain injury in humans. Although we could detect clear alteration of pyruvate metabolism in the injured brain, biological interpretation of the imaging biomarker needs to be careful and requires further clarification. First, production of [1-^{13}C]lactate signal reflects both metabolic flux from pyruvate to lactate and isotopic chemical exchange between pyruvate and lactate (Kennedy et al., 2012). The latter can be significantly affected by the intrinsic lactate pool size (Hurd et al., 2013). Second, unlike [^{13}C]HCO_3^-, [1-^{13}C]lactate signal detected in the brain is not exclusively produced by brain tissues as [1-^{13}C]lactate produced in the vasculature or other organs (Wespi et al., 2018; Xu et al., 2011) can be delivered to the brain. Moreover, although lactate is a preferred energy substrate for neurons (Bélanger et al., 2011; Magistretti and Allaman, 2018), it is likely that the excessive cerebral presence of hyperpolarized pyruvate results in cellular transport of pyruvate (and lactate) into both neurons and glia via monocarboxylate transporters. The large spatial resolution is another limitation of the study. Although the large voxel size was helpful to achieve reliable detection of HCO_3^-, it was unavoidable to experience partial volume effects in the ^{13}C images. Imaging with improved spatial resolution will be required for accurate regional assessment of TBI metabolism and to reduce the partial volume effects. The statistical analysis was not performed in this pilot study primarily due to the small number of subjects and the difficulty of patient recruitments in such an acute stage. Considering the diversity of brain injury types and the complexity of secondary

injuries, studies with a larger number of patients with longitudinal follow-ups will be necessary for further evaluation of the imaging technique and for systematic characterization of the metabolic alterations.

Resource Availability

Lead Contact

Further information and requests for resources should be directed to and will be fulfilled by the Lead Contact, Jae Mo Park (jaemo.park@utsouthwestern.edu).

Materials Availability

This study did not generate new unique reagents or materials.

Data and Code Availability

Original/source data or images in the paper is available upon request.

METHODS

All methods can be found in the accompanying Transparent Methods supplemental file.

SUPPLEMENTAL INFORMATION

Supplemental Information can be found online at https://doi.org/10.1016/j.isci.2020.101885.

ACKNOWLEDGMENTS

Funding: The Texas Institute for Brain Injury and Repair of Peter O'Donnell Jr. Brain Institute; The Mobility Foundation; National Institutes of Health of the United States (1R01NS107409-01A1, 5P41EB015908-32, 1S10OD018468-01); The Welch Foundation (I-2009-20190330). **Personnel Support**: We appreciate the research nurses and the MR technicians of the Advanced Imaging Research Center at UT Southwestern—Lucy Christie, Jeannie Baxter, Kelley Derner, Maida Tai, and Salvador Pena.

AUTHOR CONTRIBUTIONS

M.C.P., C.J.M., and J.M.P. designed research; E.P.H., M.C.P., S.B., C.J.M., and J.M.P. recruited patients; E.P.H., C.E.H., J.L., J.R., G.D.R., C.R.M., and J.M.P. performed research; E.P.H., M.C.P., C.J.M., and J.M.P. analyzed data; E.P.H., M.C.P., C.R.M., C.J.M., and J.M.P. wrote the paper.

DECLARATION OF INTERESTS

G.D.R. is an employee of GE Healthcare.

Received: July 20, 2020
Revised: October 25, 2020
Accepted: November 25, 2020
Published: December 18, 2020

REFERENCES

Ardenkjaer-Larsen, J.H., Fridlund, B., Gram, A., Hansson, G., Hansson, L., Lerche, M.H., Servin, R., Thaning, M., and Golman, K. (2003). Increase in signal-to-noise ratio of > 10,000 times in liquid-state NMR. Proc. Natl. Acad. Sci. U S A *100*, 10158–10163.

Bartnik-Olson, B.L., Harris, N.G., Shijo, K., and Sutton, R.L. (2013). Insights into the metabolic response to traumatic brain injury as revealed by (13)C NMR spectroscopy. Front. Neuroenergetics *5*, 8.

Bergsneider, M., Hovda, D.A., Shalmon, E., Kelly, D.F., Vespa, P.M., Martin, N.A., Phelps, M.E., McArthur, D.L., Caron, M.J., Kraus, J.F., and Becker, D.P. (1997). Cerebral hyperglycolysis following severe traumatic brain injury in humans: a positron emission tomography study. J. Neurosurg. *86*, 241–251.

Bélanger, M., Allaman, I., and Magistretti, P.J. (2011). Brain energy metabolism: focus on astrocyte-neuron metabolic cooperation. Cell Metab. *14*, 724–738.

Brooks, G.A., and Martin, N.A. (2015). Cerebral metabolism following traumatic brain injury: new discoveries with implications for treatment. Front. Neurosci. *8*, 408.

Corps, K.N., Roth, T.L., and McGavern, D.B. (2015). Inflammation and neuroprotection in traumatic brain injury. JAMA Neurol. *72*, 355–362.

DeVience, S.J., Lu, X., Proctor, J., Rangghran, P., Melhem, E.R., Gullapalli, R., Fiskum, G.M., and Mayer, D. (2017). Metabolic imaging of energy metabolism in traumatic brain injury using hyperpolarized [1-13C]pyruvate. Sci. Rep. *7*, 1907.

Dusick, J.R., Glenn, T.C., Lee, W.N.P., Vespa, P.M., Kelly, D.F., Lee, S.M., Hovda, D.A., and Martin, N.A. (2007). Increased pentose phosphate pathway flux after clinical traumatic brain injury: a [1,2-13C2]glucose labeling study in humans. J. Cereb. Blood Flow Metab. *27*, 1593–1602.

Gordon, J.W., Chen, H.-Y., Autry, A., Park, I., Van Criekinge, M., Mammoli, D., Milshteyn, E., Bok, R., Xu, D., Li, Y., et al. (2019). Translation of

Carbon-13 EPI for hyperpolarized MR molecular imaging of prostate and brain cancer patients. Magn. Reson. Med. *81*, 2702–2709.

Greco, T., Vespa, P.M., and Prins, M.L. (2020). Alternative substrate metabolism depends on cerebral metabolic state following traumatic brain injury. Exp. Neurol. *329*, 113289.

Guglielmetti, C., Chou, A., Krukowski, K., Najac, C., Feng, X., Riparip, L.-K., Rosi, S., and Chaumeil, M.M. (2017). In vivo metabolic imaging of Traumatic Brain Injury. Sci. Rep. *7*, 17525.

Hurd, R.E., Spielman, D., Josan, S., Yen, Y.-F., Pfefferbaum, A., and Mayer, D. (2013). Exchange-linked dissolution agents in dissolution-DNP (13) C metabolic imaging. Maregn Reson. Med. *70*, 936–942.

Hutchinson, P.J., O'Connell, M.T., Seal, A., Nortje, J., Timofeev, I., Al-Rawi, P.G., Coles, J.P., Fryer, T.D., Menon, D.K., Pickard, J.D., and Carpenter, K.L.H. (2009). A combined microdialysis and FDG-PET study of glucose metabolism in head injury. Acta Neurochir (Wien) *151*, 51–61, discussion 61.

Jalloh, I., Carpenter, K.L.H., Helmy, A., Carpenter, T.A., Menon, D.K., and Hutchinson, P.J. (2015). Glucose metabolism following human traumatic brain injury: methods of assessment and pathophysiological findings. Metab. Brain Dis. *30*, 615–632.

Kennedy, B.W.C., Kettunen, M.I., Hu, D.-E., and Brindle, K.M. (2012). Probing lactate dehydrogenase activity in tumors by measuring hydrogen/deuterium exchange in hyperpolarized l-[1-(13)C,U-(2)H]lactate. J. Am. Chem. Soc. *134*, 4969–4977.

Kim, S., Han, S.C., Gallan, A.J., and Hayes, J.P. (2017). Neurometabolic indicators of mitochondrial dysfunction in repetitive mild traumatic brain injury. Concussion *2*, CNC48.

Lee, C.Y., Soliman, H., Geraghty, B.J., Chen, A.P., Connelly, K.A., Endre, R., Perks, W.J., Heyn, C., Black, S.E., and Cunningham, C.H. (2019). Lactate topography of the human brain using hyperpolarized 13C-MRI. Neuroimage *204*, 116202.

Magistretti, P.J., and Allaman, I. (2018). Lactate in the brain: from metabolic end-product to signalling molecule. Nat. Rev. Neurosci. *19*, 235–249.

Moro, N., Ghavim, S.S., Harris, N.G., Hovda, D.A., and Sutton, R.L. (2016). Pyruvate treatment attenuates cerebral metabolic depression and neuronal loss after experimental traumatic brain injury. Brain Res. *1642*, 270–277.

Shank, R.P., Bennett, G.S., Freytag, S.O., and Campbell, G.L. (1985). Pyruvate carboxylase: an astrocyte-specific enzyme implicated in the replenishment of amino acid neurotransmitter pools. Brain Res. *329*, 364–367.

Smith, D.H., Johnson, V.E., and Stewart, W. (2013). Chronic neuropathologies of single and repetitive TBI: substrates of dementia? Nat. Rev. Neurol. *9*, 211–221.

Varrone, A., Asenbaum, S., Vander Borght, T., Booij, J., Nobili, F., Någren, K., Darcourt, J., Kapucu, O.L., Tatsch, K., Bartenstein, P., and Van Laere, K.; European Association of Nuclear Medicine Neuroimaging Committee (2009). EANM procedure guidelines for PET brain imaging using [18F]FDG, version 2. Eur. J. Nucl. Med. Mol. Imaging *36*, 2103–2110.

Viglianti, B.L., Wong, K.K., Wimer, S.M., Parameswaran, A., Nan, B., Ky, C., Townsend, D.M., Rubello, D., Frey, K.A., and Gross, M.D. (2017). Effect of hyperglycemia on brain and liver 18F-FDG standardized uptake value (FDG SUV) measured by quantitative positron emission tomography (PET) imaging. Biomed. Pharmacother. *88*, 1038–1045.

Wespi, P., Steinhauser, J., Kwiatkowski, G., and Kozerke, S. (2018). Overestimation of cardiac lactate production caused by liver metabolism of hyperpolarized [1-13 C]pyruvate. Magn. Reson. Med. *80*, 1882–1890.

Xiong, Y., Zhang, Y., Mahmood, A., and Chopp, M. (2015). Investigational agents for treatment of traumatic brain injury. Expert Opin. Investig. Drugs *24*, 743–760.

Xu, T., Mayer, D., Gu, M., Yen, Y.-F., Josan, S., Tropp, J., Pfefferbaum, A., Hurd, R., and Spielman, D. (2011). Quantification of in vivo metabolic kinetics of hyperpolarized pyruvate in rat kidneys using dynamic 13C MRSI. NMR Biomed. *24*, 997–1005.

iScience, Volume *23*

Supplemental Information

Imaging Acute Metabolic Changes in Patients with Mild Traumatic Brain Injury Using Hyperpolarized [1-^{13}C]Pyruvate

Edward P. Hackett, Marco C. Pinho, Crystal E. Harrison, Galen D. Reed, Jeff Liticker, Jaffar Raza, Ronald G. Hall, Craig R. Malloy, Surendra Barshikar, Christopher J. Madden, and Jae Mo Park

Supplementary Information

Transparent Methods

Human subjects and patient recruitment criteria

This study was approved by the local Institutional Review Board (IRB) of the University of Texas Southwestern Medical Center (IRB#: STU 072017-009; ClinicalTrials.gov NCT03502967). A written and informed consent was obtained from all the study participants. The imaging protocol was fully compliant with HIPPA regulation. Patients between the age of 18-60 years old in good general health were screened for enrollment if they had sustained a mild injury to the head with no structural brain damage detected in any CT scans within 10 days of trauma. Patients were further screened to exclude any confounding comorbidities including a history of mental illness, history of substance abuse, and other major medical conditions. Patients with known prior cardiovascular or neurological disease were excluded.

$^{1}H/^{13}C$ MRI protocol

All the studies were performed using a clinical SPINlab^{TM} polarizer (GE Healthcare, Waukesha, WI USA), a 3T wide-bore MR scanner (GE Healthcare, 750w Discovery), and a $^{13}C/^{1}H$ dual-frequency (^{1}H: quadrature transmit/receive, ^{13}C: quadrature transmit/8-channel phased array receive) nested-design radiofrequency (RF) head coil (Clinical MR Solutions, Brookfield, WI USA) (Ma et al., 2019). Both study participants in this report were recruited at the Parkland Health and Hospital System Emergency Department, a UT Southwestern-affiliated hospital in Dallas. When admitted, a full workup that includes primary and secondary trauma survey, blood tests, and CT imaging of head and C-spine was initiated and the CT scans showed no evidence of intracranial injury for either patient. The patients were released with minor laceration care and brought in for research imaging. The subjects were imaged with a brain MR protocol, which includes an injection of hyperpolarized [1-^{13}C]pyruvate (IND#: 133229). The hyperpolarized pyruvate solution was injected after a two-dimensional T_2-weighted fluid attenuated inversion recovery (FLAIR) scan. For ^{13}C acquisition, a volume of 250-mM hyperpolarized pyruvate

corresponding to a 0.1 mmol/kg dose was injected, followed by a 25-mL saline flush. The injection rate was 5 mL/sec. A single-slice two-dimensional (2D) dynamic spiral chemical shift imaging (spiral CSI) was used for dynamic imaging of hyperpolarized ^{13}C signals (Park et al., 2012; 2019).

Each subject was scanned by a 3-plane ^{1}H gradient echo sequence (fast GRE; field of view [FOV] = 32 cm, echo time [TE] = 1.1 msec, repetition time [TR] = 3.6 msec, slice thickness = 10 mm), followed by a 2D axial T_2-weighted fluid-attenuated and inversion recovery (T_2w FLAIR; FOV = 24 cm × 24 cm, TE = 144.7 ms, TR = 8 sec, inversion time [TI] = 2163 msec, slice thickness = 5 mm, number of slices = 16, flip-angle [FA] = 160°) as a basic assessment of axonal/parenchymal injuries that are typical manifestations of trauma. Prior to ^{13}C imaging, B_0 inhomogeneity of the target ^{13}C slice was minimized using a single-voxel ^{1}H point-resolved spectroscopy (PRESS) sequence by adjusting shim gradients up to 1st order. For ^{13}C metabolic imaging, ^{13}C spiral chemical shift imaging (FOV = 24 cm × 24 cm, matrix size = 16 × 16, slice thickness = 3 cm, variable FA up to 30° per timepoint, TR = 5 sec, 7 spatial interleaves of spiral readout, spectral width = 814 Hz, 48 echoes) was used with a bolus injection of hyperpolarized [1-^{13}C]pyruvate. The ^{13}C scan was initiated 5-sec after the start of injection. The ^{13}C transmit power was pre-calibrated with a gadolinium-doped 0.4-M spherical [^{13}C]HCO_3^- phantom (diameter = 18 cm). After the ^{13}C acquisition, ^{1}H images were further acquired from each subject for mapping brain anatomy: T_1-weighted FLAIR (FOV = 24 cm × 24 cm, TE = 9.4 msec, TR = 3109 msec, inversion time [TI] = 1215 msec, slice thickness = 5 mm, number of slices = 16, FA = 142°), a 3D pseudo-continuous arterial spin labeling (ASL) sequence with stack of spiral readouts (FOV = 24 cm × 24 cm × 16.2 cm, TE = 9.9 msec, TR = 6733 msec, post-labeling delay = 2025 msec, 3 averages, matrix size = 512/interleave, 8 interleaves, flip angle = 90°). ASL was performed to identify vascular imbalance of the injured region (e.g., hypoperfusion).

Reconstruction of ^{13}C data

All ^{13}C data were reconstructed using MATLAB (Mathworks, Natick, MA). After apodization by a 10-Hz Gaussian filter, the raw data were zero-filled in spectral and spatial domains by a factor of 4,

followed by an FFT along time. Subsequently, the Hanning filter ($\alpha = 0.66$) was applied and gridding onto Cartesian coordinate and applying a 2D spatial inverse FFT were performed. Metabolite maps of pyruvate, pyruvate-hydrate, lactate, and bicarbonate were generated by integrating the corresponding metabolite peaks in the absorption mode spectra, and normalized to the total ^{3}C map, which is sum of pyruvate, pyruvate-hydrate, lactate, and bicarbonate maps to compensate the spatial heterogeneity in HP pyruvate delivery and ^{13}C receive profile. The final axial metabolite maps were overlaid on the corresponding ^{1}H MRI for anatomical reference.

For quantitative assessment of each brain metabolite, spectra were averaged over selected regions of interest (ROIs) before integrating individual peaks. Two regions of interest (ROIs) were selected; one in injured brain region (ROI_{TBI}) and another brain ROI in the contralateral hemisphere (ROI_{CTL}). Each metabolite was separately reconstructed and phase was corrected up to 1^{st} order for display of the reconstructed spectra. Each metabolite was normalized to the sum of total ^{13}C-labeled metabolite (TC) signal.

Supplemental References

Ma, J., Hashoian, R.S., Sun, C., Wright, S.M., Ivanishev, A., Lenkinski, R.E., Malloy, C.R., Chen, A.P., Park, J.M., 2019. Development of 1H/13C RF head coil for hyperpolarized 13C imaging of human brain, Presented at the International Society of Magnetic Resonance in Medicine, Montreal, Canada, #568.

Park, J.M., Josan, S., Jang, T., Merchant, M., Yen, Y.-F., Hurd, R.E., Recht, L., Spielman, D.M., Mayer, D., 2012. Metabolite kinetics in C6 rat glioma model using magnetic resonance spectroscopic imaging of hyperpolarized [1-(13)C]pyruvate. Magn Reson Med 68, 1886–1893. doi:10.1002/mrm.24181

Park, J.M., Liticker, J., Harrison, C.E., Reed, G.D., Hever, T., Ma, J., Martin, R., Mayer, D., Hashoian, R.S., Madden, C.J., Pinho, M., Malloy, C.R., 2019. Feasibility and reproducibility of imaging brain metabolism using hyperpolarized 13C pyruvate in humans, Presented at the International Society of Magnetic Resonance in Medicine, Montreal, Canada, #4311.